JPEDAV (2015) 36:218–223
DOI: 10.1007/s11669-015-0375-5
1547-7037 ©ASM International

Experimental Phase Diagram of the Al–Mo–Gd Ternary System at 773 K

Hao Liu, Yanfang Pan, Chenghuang Tang, Moumiao Liu, Xiaoxian Chen, Wenchao Yang, Hongqun Tang, and Yongzhong Zhan

(Submitted October 20, 2014; in revised form March 2, 2015; published online March 19, 2015)

The nature of the isothermal region of the Al–Mo–Gd ternary system at 773 K has been established by analysis of quenched samples, annealed for 6 weeks, by use of x-ray powder diffraction and scanning electron microscopy equipped with energy-dispersive analysis. Two ternary phases, $Al_{43}Mo_4Gd_6$ and Al_4Mo_2Gd were observed. Ten binary phases, including $Al_{17}Mo_4$ rather than Al_4Mo, were present at 773 K in the Al–Mo system. The ranges of homogeneity of the $AlMo_3$ and Al_8Mo_3 phases were 7.5 and 1 at.%, respectively. According to results obtained from the disappearing-phase method, the maximum solubility of Al in Mo is approximately 16 at.%.

Keywords Al–Mo–Gd ternary system, phase diagram, rare earth alloys, X-ray diffraction

1. Introduction

Over the past three decades, Al-based amorphous alloys have attracted much attention, because of their unique combination of ultrahigh strength, excellent corrosion resistance, and high ductility.[1,2] Unfortunately, poor glass-forming ability (GFA) limits commercial application of Al-based amorphous alloys.[3] Alloying additions are widely used to improve GFA of metallic alloys.[4] High glass formability occurs as a result of negative heat of formation of the alloy components, different atomic size ratios of the components, and use of multicomponent systems.[5,6] Al–TM–RE systems have GF potential. First, the three components of Al–RE–TM alloys have negative heats of mixing with each other.[7] Second, bulk metallic glasses (BMG) can be broadly categorized into two types, the major atom–small atom–large atom (MSL) class and the large atom–small atom or small atom–large atom (LS/SL) class. The Al–TM–RE system can be classified as an MSL class with substantially different atomic size ratios.[6] Third, the appropriate composition for formation of solute-centered quasi-equivalent clusters about rare earth (RE) and transition metal (TM) elements is structurally favorable for retarding formation of α-Al and enhancing the resistance to crystallization of supercooled liquids.[8,9] A series of related studies have been reported.[10,11] Yang et al.[12] were the first to successfully design Al-rich (86 at.% Al) bulk metallic glasses by addition of RE and TM in appropriate proportions. Other research[13–15] has shown that Al–TM–RE alloys of appropriate composition containing more than 80% Al have outstanding ductility and exceptional tensile strength.

Addition of RE elements and transition elements also contributes to amelioration of the mechanical behavior and elevated-temperature applications of traditional aluminium alloys. The strengthening occurs as a result of the distribution of intermetallic dispersoids and the formation of high-melting-point compounds.[16,17]

Although Al–TM–Gd phase diagrams at 773 K have been reported for TM = Cr, Ni, Ti, V, and Cu,[18–22] that of Al–Mo–Gd, also a Al–TM–Gd system, has not been reported, although the presence at 773 K of the ternary compounds $Al_{43}Mo_4Gd_6$ and Al_4Mo_2Gd has been reported.[23,24] In the work discussed in this paper, the Al–Mo–Gd ternary system at 773 K was characterized experimentally to investigate the interactions between the elements Al, Mo, and Gd which may be conducive to the design of new types of Al-based amorphous alloys or new Al alloys.

2. Literature Data

Phase equilibrium data were obtained for each binary phase diagram of the Al–Mo–Gd ternary system. In 2010, Okamoto[25] updated the Al–Mo phase diagram by summarizing previous literature which confirmed the presence of ten intermetallic phases ($AlMo_3$, AlMo, $Al_{63}Mo_{37}$, Al_8Mo_3, Al_3Mo, Al_4Mo, $Al_{17}Mo_4$, $Al_{22}Mo_5$, Al_5Mo, and $Al_{12}Mo$). Schuster and Ipser[26] emphasized three modifications of Al_5Mo, denoted Al_5Mo (h), Al_5Mo (h′) and Al_5Mo (r), respectively. According to Eumann et al.,[27] six compounds, $AlMo_3$, Al_8Mo_3, $Al_{17}Mo_4$, $Al_{22}Mo_5$, Al_5Mo, and $Al_{12}Mo$ were stable at moderate temperatures, although Schuster and Ipser[26] did not confirm the presence of $Al_{22}Mo_5$ at 773 K.

Basic data for the Al–Gd system were obtained by Gschneidner and Calderwood,[28] Saccone et al.,[29] and

Hao Liu, Yanfang Pan, Chenghuang Tang, Moumiao Liu, Xiaoxian Chen, Wenchao Yang, Hongqun Tang, and **Yongzhong Zhan,** College of Materials Science and Engineering, Guangxi University, Nanning 530004 Guangxi, People's Republic of China. Contact e-mails: zyzmatres@aliyun.com and zyzmatres@163.com.

Elliott and Shunk.[30] Five intermetallic phases ($AlGd_2$, Al_2Gd_3, AlGd, Al_2Gd, and Al_3Gd) were identified as stable; two unstable phases, Al_4Gd [31] and $Al_{17}Gd_2$,[32] have also been reported.

No intermetallic compounds have been reported for the binary Gd–Mo system. Low terminal solubilities have been reported for this system.[33,34]

Only two ternary aluminides have been reported for the Al–Mo–Gd system. Fornasini and Palenzona[24] reported the crystal structure of the Al_4Mo_2Gd phase in 1976, and the structure of $Al_{43}Mo_4Gd_6$ was determined by Niemann and Jeitschko.[23]

Details of these phases, and of the stable phases discovered in this work are listed in Table 1.

3. Experimental Procedure

All the samples were prepared in an arc-melting furnace. The nominal compositions of the alloys were determined on the basis of the predicted three-phase regions. High-purity metals, aluminium pieces (99.99 wt.%), molybdenum rods (99.9 wt.%), and gadolinium pieces (99.9 wt.%), were used as starting materials to ensure the accuracy of the experiments. One-hundred and seventy samples were prepared. The weight of each sample was 2 g. Electric argon-arc welding with a tungsten electrode was performed with the sample in a water-cooled copper vessel. Each sample was remelted at least five times (weight loss $<1\%$) to ensure compositional uniformity. The samples were then placed in quartz tubes (10 mm diameter), which were sealed under high vacuum, and annealed at 773 K for 6 weeks in an electric resistance furnace. After heat-treatment, the samples were quenched in liquid nitrogen, so the rapid cooling preserved the composition of the material obtained at 773 K. All the equilibrated samples were subjected to x-ray diffraction (XRD) analysis with a Rigaku D/Max 2500 V diffractometer operated at 40 kV and 200 mA with a copper target. XRD data were analyzed by use of Jade 6.5 software and Pearson's Handbook on Crystallographic Data. Scanning electron microscopy (SEM) with energy-dispersive analysis (EDS) (Hitachi S-3400) was used to examine the microstructure of samples.

4. Results and Discussion

4.1 Binary Phase Analysis

Five binary Al–Mo phases were observed at 773 K: $AlMo_3$, Al_8Mo_3, $Al_{17}Mo_4$, Al_5Mo, and $Al_{12}Mo$. Five binary Al–Gd phases were observed at 773 K: Al_3Gd, Al_2Gd, AlGd, Al_2Gd_3, and $AlGd_2$. No binary Mo-Gd compound was found.

On the basis of the crystallographic data of Grin et al.[35] and Fornasini and Palenzona,[24] XRD patterns of $Al_{17}Mo_4$

Table 1 Crystallographic data for phases related to the Al–Mo–Gd system

Compound	Prototype	Pearson symbol	Space group	Lattice constants, nm			Stable phase in this work?	Ref.
				a	*b*	*c*		
Al	Cu	cF4	$Fm\bar{3}m$	0.4050(2)	–	–	✔	[27]
Mo	w	cI2	$Im\bar{3}m$	0.31451	–	–	✔	[28]
Gd	Mg	hP2	$P6_3/mmc$	0.36330	–	0.57739	✔	[29]
$AlMo_3$	Cr_3Si	cP8	$Pm\bar{3}m$	0.4950	–	–	✔	[28]
AlMo	w	cI2	$Im\bar{3}m$	0.3098	–	–	–	[30]
$Al_{63}Mo_{37}$	–	–	–	–	–	–	–	[30]
Al_8Mo_3	Al_8Mo_3	mC22	$C2/m$	0.9208(3)	0.36378(3)	1.0065(3)	✔	[31]
Al_3Mo	Al_3Mo	mC32	Cm	1.6396	0.3594(1)	0.8386(4)	–	[16]
Al_4Mo	Al_4W	mC30	Cm	0.5225(5)	1.7768(5)	0.5225(5)	–	[32]
$Al_{17}Mo_4$	$Al_{17}Mo_4$	mC84	$C2$	0.9158(1)	0.49323(8)	2.8935(5)	✔	[33]
$Al_{22}Mo_5$	$Al_{22}Mo_5$	oF216	$Fdd2$	7.382(3)	0.9161(3)	0.4933(2)	–	[33]
Al_5Mo (h)	Al_5W	hP12	$P6_3$	0.4912(2)	–	0.8860(4)	–	[16]
Al_5Mo (h′)	Al_5Mo	hP60	$P3$	0.4933(1)	4.398(9)	–	–	[16]
Al_5Mo (r)	Al_5Mo	hR12	$R\bar{3}c$	0.4951(1)	2.623(2)	–	✔	[16]
$Al_{12}Mo$	$Al_{12}W$	cI26	$Im\bar{3}$	0.75815	–	–	✔	[34]
$AlGd_2$	Co_2Si	oP12	$Pnma$	0.657	0.509	0.9505	✔	[35]
Al_2Gd_3	Al_2Gd_3	tP20	$P4_2nm$	0.8344(4)	–	0.7656(6)	✔	[36]
AlGd	AlDy	oP16	$Pbcm$	0.5888	1.1527	0.5656	✔	[36]
Al_2Gd	Cu_2Mg	cF24	$Fd\bar{3}m$	0.79002	–	–	✔	[37]
Al_3Gd	Ni_3Sn	hP8	$P6_3/mmc$	0.6332	–	0.4600	✔	
Al_4Gd	Al_4U	oI20	$Imma$	0.4442(1)	0.6316(1)	1.3739(3)	–	[21]
$Al_{17}Gd_2$	$Ni_{17}Th_2$	hP38	$P6_3/mmc$	0.8869	–	0.9711	–	[22]
$Al_{43}Mo_4Gd_6$	$Al_{43}Mo_4Ho_6$	hP106	$P6_3/mcm$	1.1011(1)	–	1.7771(2)	✔	[26]
Al_4Mo_2Gd	Al_4Mo_2Yb	tI14	$I4/mmm$	0.6780(4)	–	0.5331(4)	✔	[25]

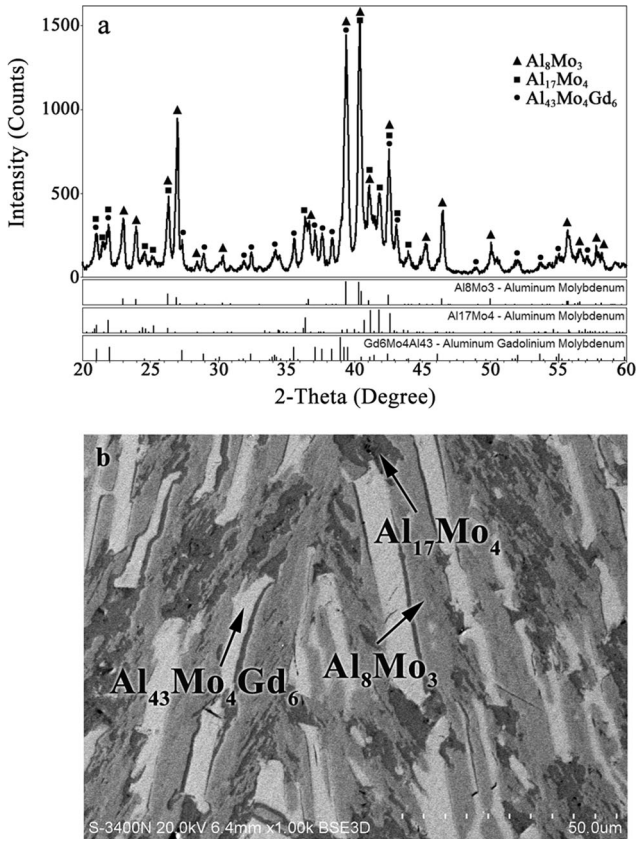

Fig. 1 XRD pattern (a) and SEM micrograph (b) of the equilibrated sample (78 at.% Al, 20 at.% Mo, and 2 at.% Gd) containing Al_8Mo_3, $Al_{17}Mo_4$, and $Al_{43}Mo_4Gd_6$

and Al_4Mo_2Gd were identified by the powder cell software. Brewer et al.[36] reported five phases ($Al_{12}Mo$, Al_5Mo, Al_4Mo, Al_8Mo_3, $AlMo_3$) at 773 K. However, the Al_4Mo phase was replaced by $Al_{17}Mo_4$ in results published by EuMann et al.[27] and Schuster and Ipser.[26] Moreover, in the study by Potzschke et al.,[37] the Al_4Mo phase decomposed below 993 K. In our work we identified five phases, $Al_{12}Mo$, Al_5Mo, $Al_{17}Mo_4$, Al_8Mo_3, and $AlMo_3$, at 773 K, in good agreement with the results of EuMann et al.[27] and Schuster and Ipser.[26] In Fig. 1(a), black triangles, black squares, and solid black circles are used to mark the peaks of Al_8Mo_3, $Al_{17}Mo_4$, and $Al_{43}Mo_6Gd_4$, respectively. The PDF cards of the other phases, i.e. Al_4Mo and Al_5Mo, did not match the XRD result. It is obvious that each phase has unique peaks which unequivocally prove the presence of the corresponding phase. When the peaks of relevant phases overlap, these are marked, in order, from high to low in accordance with the diffraction peak intensities on the PDF cards of corresponding phases. The XRD pattern in Fig. 1(a) and the SEM micrograph of the ternary alloy of composition 78 at.% Al, 20 at.%, 2 at.% Gd in Fig. 1(b)

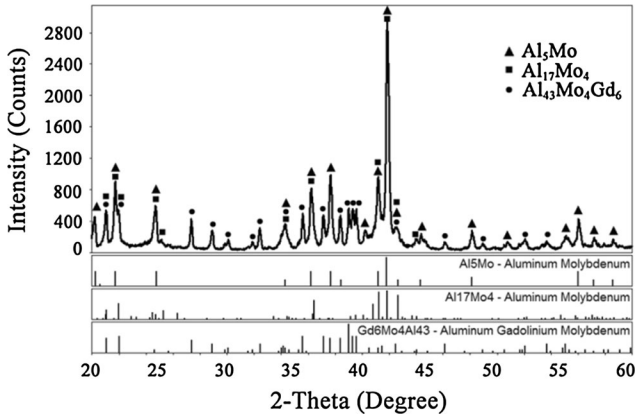

Fig. 2 XRD pattern of the equilibrated sample (82 at.% Al, 15 at.% Mo, and 3 at.% Gd) containing Al_5Mo, $Al_{17}Mo_4$, and $Al_{43}Mo_4Gd_6$

indicate the presence of the equilibrium phase $Al_8Mo_3 + Al_{17}Mo_4 + Al_{43}Mo_4Gd_6$, which confirms the occurrence of the binary phase $Al_{17}Mo_4$ at 773 K. Moreover, the XRD pattern of the equilibrated alloy containing 82 at.% Al, 15 at.% Mo, and 3 at.% Gd is indicative of the equilibrium of three phases $Al_5Mo + Al_{17}Mo_4 + Al_{43}Mo_4Gd_6$ at 773 K, as shown in Fig. 2. The EDS results for relevant samples are shown in Table 2. The EDS data were acquired by scanning small areas; each measurement was performed three times and the average value was calculated. The EDS results also confirm the presence of $Al_{17}Mo_4$. The uncertainty of some measurements can be attributed to the presence of solid solutions. These still provide effective references for the XRD patterns, however. By analysis of related results, the presence of $Al_{17}Mo_4$, rather than Al_4Mo, was confirmed at 773 K.

4.2 Ternary Compounds

Two ternary compounds, $Al_{43}Mo_4Gd_6$ and Al_4Mo_2Gd, were detected in this work, in good agreement with the literature. Figure 3(a) shows that the equilibrated sample $Al_{86}Mo_{12}Gd_2$ annealed at 773 K consists of three phases, Al_5Mo, $Al_{43}Mo_4Gd_6$, and $Al_{12}Mo$. The microstructure of the sample examined by SEM and EDS clearly indicates the presence of these three phases: the light gray phase is Al_5Mo, the white phase is $Al_{43}Mo_4Gd_6$, and the dark grey phase is $Al_{12}Mo$, as indicated in Fig. 3(b). Figure 4 clearly indicates that the Al_4Mo_2Gd phase is located in the $AlMo_3 + Al_8Mo_3 + Al_4Mo_2Gd$ three-phase region.

4.3 Solid Solubility

Solid solubility in this isothermal region was determined by use of the disappearing-phase method, each experiment being performed in duplicate. Figure 5 shows that the binary

Table 2 Results from EDS for relevant samples

Sample	Phase	Composition of phases by EDS, at.%		
		Al	Mo	Gd
$Al_{72}Mo_{20}Gd_2$	Al_8Mo_3	71.75	27.65	0.60
	$Al_{17}Mo_4$	80.15	19.85	0.00
	$Al_{43}Mo_4Gd_6$	78.61	8.99	12.41
$Al_{82}Mo_{15}Gd_3$	Al_5Mo	81.28	18.11	0.61
	$Al_{17}Mo_4$	80.54	19.46	0.00
	$Al_{43}Mo_4Gd_6$	78.35	8.89	12.76

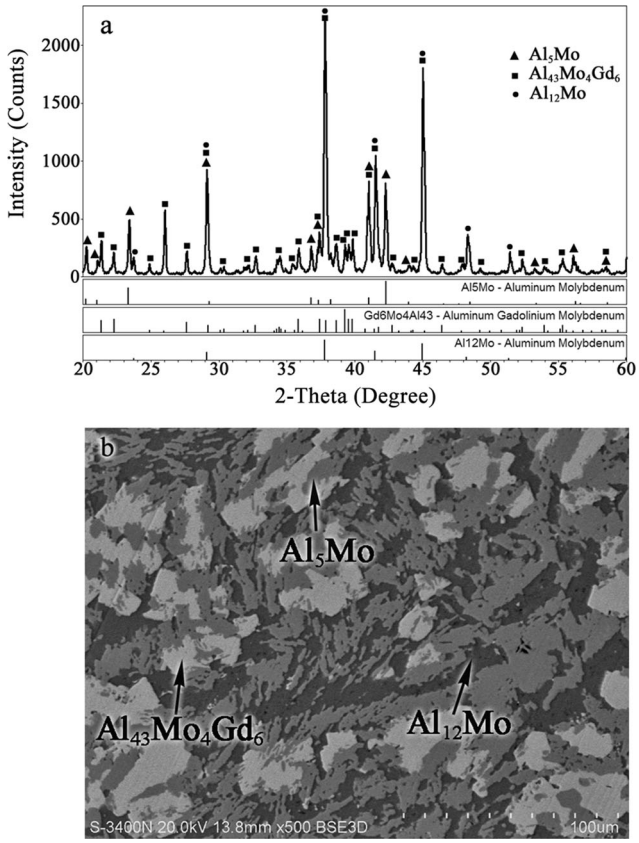

Fig. 3 XRD pattern (a) and SEM micrograph (b) of the equilibrated sample (86 at.% Al, 12 at.% Mo, and 2 at.% Gd) containing Al_5Mo, $Al_{43}Mo_4Gd_6$, and $Al_{12}Mo$

compound $AlMo_3$ has a distinct homogeneity range from 21 to 28.5% Al at 773 K. When the aluminium content was outside this range the peak arising from the other phase was observed. In this way the maximum solubility of Al in Al_8Mo_3 was confirmed to be approximately 1 at.% (approx. 72–73% Al) at 773 K, as shown in Fig. 6; this was consistent with the reported Al–Mo binary phase diagram.[27] The solid solubility of Al in Mo was determined to be approximately 16 at.%.

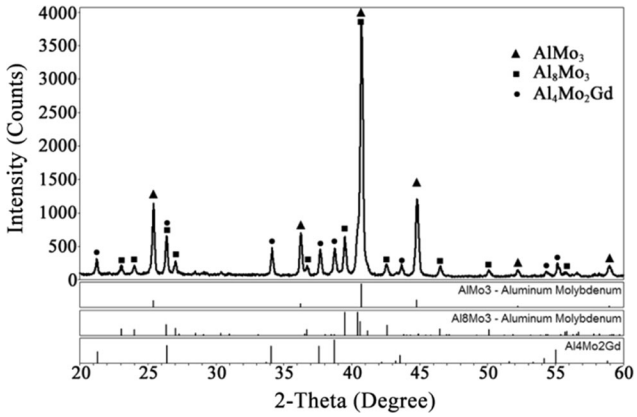

Fig. 4 XRD patterns of the equilibrated alloy (39 at.% Al, 59 at.% Mo, and 2 at.% Gd) containing $AlMo_3$, Al_8Mo_3, and Al_4Mo_2Gd

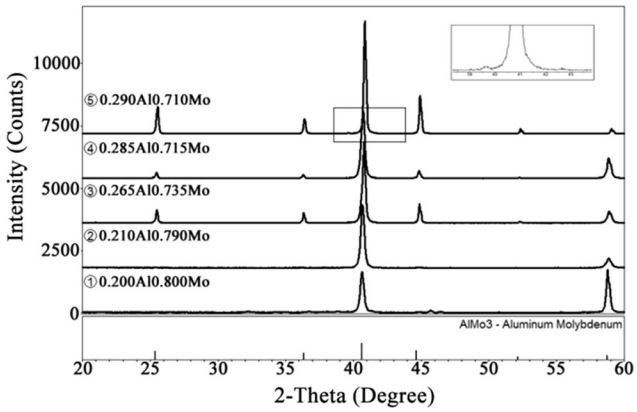

Fig. 5 XRD patterns of equilibrated alloys Al_xMo_{1-x} (x = 0.200, 0.210, 0.265, 0.285, 0.290)

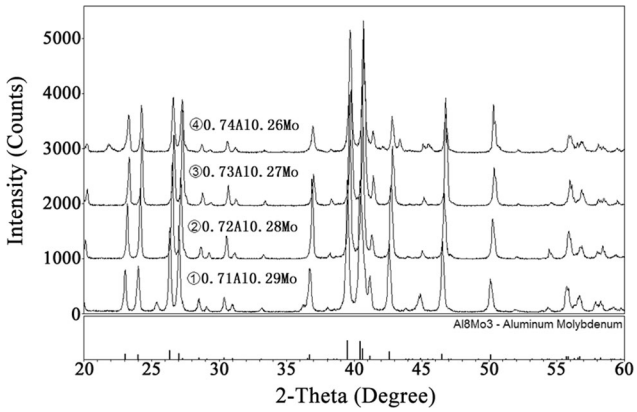

Fig. 6 XRD patterns of equilibrated alloys Al_xMo_{1-x} (x = 0.71, 0.72, 0.73, 0.74)

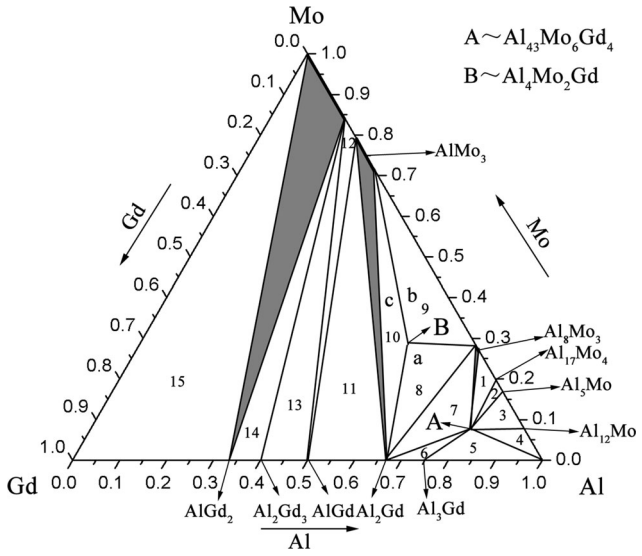

Fig. 7 Isothermal region of the Al–Mo–Gd system at 773 K

Table 3 Summary of the three-phase regions of the Al–Mo–Gd system at 773 K

	Nominal composition, at.%			
Phase region	**Al**	**Mo**	**Gd**	**Phases**
1	78	20	2	Al_8Mo_3 + $Al_{17}Mo_4$ + $Al_{43}Mo_6Gd_4$
2	82	15	3	$Al_{17}Mo_4$ + Al_5Mo + $Al_{43}Mo_6Gd_4$
3	86	12	2	Al_5Mo + $Al_{12}Mo$ + $Al_{43}Mo_6Gd_4$
4	92	6	2	Al + $Al_{12}Mo$ + $Al_{43}Mo_6Gd_4$
5	92	4	4	Al + Al_3Gd + $Al_{43}Mo_6Gd_4$
6	74	2	24	Al_2Gd + Al_3Gd + $Al_{43}Mo_6Gd_4$
7	71	8	21	Al_2Gd + Al_8Mo_3 + $Al_{43}Mo_6Gd_4$
8	64	22	14	Al_2Gd + Al_8Mo_3 + $Al_{43}Mo_6Gd_4$
9	57	37	6	$AlMo_3$ + Al_8Mo_3 + Al_4Mo_2Gd
10	54	29	17	$AlMo_3$ + Al_2Gd + Al_4Mo_2Gd
11	44	26	30	$AlMo_3$ + Al_2Gd + AlGd
12	21	8	71	Mo + $AlMo_3$ + AlGd
13	43	51	6	Mo + AlGd + Al_2Gd_3
14	34	2	64	Mo + Al_2Gd_3 + Al_2Gd
15	12	28	60	Mo + Gd + Al_2Gd

4.4 Isothermal Region

The composition of the isothermal region of the Al–Mo–Gd system at 773 K was determined by analysis of all the samples (Fig. 7). The isothermal region consists of 15 single-phase regions, 29 binary-phase regions, and 15 ternary-phase regions. The solubility of Al in the $AlMo_3$, Al_8Mo_3, and Mo phases was measured to be approximately 7.5, 1.0, and 16.0 at.% respectively. All the details of three-phase regions of the Al–Mo–Gd ternary system at 773 K are shown in Table 3.

5. Conclusions

As part of the ternary Al–TM–RE system with excellent potential in GFA and outstanding mechanical properties, the Al–Mo–Gd ternary phase diagram at 773 K was investigated. The results show that the isothermal region consists of 15 single-phase regions, 29 binary-phase regions, and 15 ternary-phase regions. The main results are summarized as follows:

1. The presence of ten binary phases ($AlMo_3$, Al_8Mo_3, $Al_{17}Mo_4$, Al_5Mo, $Al_{12}Mo$, Al_3Gd, Al_2Gd, AlGd, Al_2Gd_3, $AlGd_2$) and two ternary phases ($Al_{43}Mo_4Gd_6$, Al_4Mo_2Gd) was confirmed at 773 K. No binary Mo–Gd phases were found at 773 K.
2. At 773 K, the homogeneity ranges of the $AlMo_3$ and Al_8Mo_3 phases are 7.5 and 1 at.%, respectively, and the solid solubility of Al in Mo is approximately 16 at.%.
3. The presence at 773 K of the controversial phase $Al_{17}Mo_4$ was confirmed experimentally.

Acknowledgments

This research work was jointly supported by the Guangxi Science and Technology Development Project (12118001-2B, 2013AA01013), and the Science and Technology Project of Guangxi Education Department (2013ZL010).

References

1. Y. He, S.J. Poon, and G.J. Shifle, Synthesis and Properties of Metallic Glasses that Contain Aluminum, *Science*, 1988, **241**(4873), p 1640-1642
2. A. Inoue, K. Ohtera, A.P. Tsai, and T. Masumoto, Aluminum-Based Amorphous Alloys with Tensile Strength Above 980 MPa (100 kg/mm^2), *Jpn. J. Appl. Phys.*, 1988, **27**(4), p 479
3. L.C. Zhou, S.J. Pang, H. Wang, and T. Zhang, Ductile Bulk Aluminum-Based Alloy with Good Glass-Forming Ability and High Strength, *Chin. Phys. Lett.*, 2009, **26**(6), p 066402
4. W.H. Wang, Roles of Minor Additions in Formation and Properties of Bulk Metallic Glasses, *Prog. Mater. Sci.*, 2007, **52**(4), p 540-596
5. A. Inoue, Stabilization of Metallic Supercooled Liquid and Bulk Amorphous Alloys, *Acta Mater.*, 2000, **48**(1), p 279-306
6. S.J. Poon, G.J. Shiflet, F. Guo, and V. Ponnambalam, Glass Formability of Ferrous- and Aluminum-Based Structural Metallic Alloys, *J. Non Cryst. Solids*, 2003, **317**(1), p 1-9
7. J. Wang, Y. Liu, S. Imhoff, N. Chen, D. Louzguine-Luzgin, A. Takeuchi, M. Chen, H. Kato, J. Perepezko, and A. Inoue, Enhance the Thermal Stability and Glass Forming Ability of Al-Based Metallic Glass by Ca Minor-Alloying, *Intermetallics*, 2012, **29**, p 35-40
8. Z.P. Chen, J.E. Gao, Y. Wu, H.X. Li, H. Wang, and Z.P. Lu, Role of Rare-Earth Elements in glass Formation of Al-Ca-Ni Amorphous Alloys, *J. Alloys Compd.*, 2012, **513**, p 387-392
9. H. Yang, J. Wang, and Y. Li, Glass Formation and Microstructure Evolution in Al-Ni-RE (RE = La, Ce, Pr, Nd and

Misch Metal) Ternary Systems, *Philos. Mag.*, 2007, **87**(27), p 4211-4228
10. K. Song, X. Bian, J. Guo, S. Wang, B.A. Sun, X. Li, and C. Wang, Effects of Ce and Mm Additions on the Glass Forming Ability of Al-Ni-Si Metallic Glass Alloys, *J. Alloys Compd.*, 2007, **440**(1), p L8-L12
11. B. Yang, J. Yao, Y. Chao, J. Wang, and E. Ma, Developing Aluminum-Based Bulk Metallic Glasses, *Philos. Mag.*, 2010, **90**(23), p 3215-3231
12. B.J. Yang, J.H. Yao, J. Zhang, H.W. Yang, J.Q. Wang, and E. Ma, Al-Rich Bulk Metallic Glasses with Plasticity and Ultrahigh Specific Strength, *Scripta Mater.*, 2009, **61**(4), p 423-426
13. R.A. Dunlap, V. Srinivas, G. Beydaghyan, and M.E. McHenry, Magnetic and Thermal Properties of Amorphous Al–Gd-TM (TM = Fe, Cu) Alloys, *J. Mater. Sci.*, 1993, **28**(11), p 2893-2897
14. A. Inoue, K. Ohtera, A.-P. Tsai, and T. Masumoto, New Amorphous Alloys with Good Ductility in Al-YM and Al-La-M (M = Fe Co, Ni or Cu) Systems, *Jpn. J. Appl. Phys*, 1988, **27**(3A), p 280
15. L. Chaosan, Z. Yongchang, and S. Changxu, New Amorphous Al-La-Y-Ni (Fe) Quaternary Alloys with Superior Strength and Ductility, *Acta Metall. Sin.*, 1993, **6**(6), p 442-446
16. C.B. Fuller, D.N. Seidman, and D.C. Dunand, Mechanical Properties of Al (Sc, Zr) Alloys at Ambient and Elevated Temperatures, *Acta Mater.*, 2003, **51**(16), p 4803-4814
17. O. Sitdikov, T. Sakai, E. Avtokratova, R. Kaibyshev, K. Tsuzaki, and Y. Watanabe, Microstructure Behavior of Al-Mg-Sc Alloy Processed by ECAP at Elevated Temperature, *Acta Mater.*, 2008, **56**(4), p 821-834
18. M. Ling, Y. Liang, S. Wei, Y. Liu, M. Pang, Y. Zhan, and Y. Du, Experimental Investigation of the Al-Cr-Gd Ternary System at 773 K, *J. Phase Equilib. Diffus.*, 2012, **33**(3), p 203-209
19. S. Delsante and G. Borzone, The Gd-Ni-Al System: Phases Formation and Isothermal Sections at 500 °C and 800°C, *Intermetallics*, 2014, **45**, p 71-79
20. V. Raghavan, Al–Gd-Ti (Aluminum-Gadolinium-Titanium), *J. Phase Equilib. Diffus.*, 2005, **26**(2), p 182-183
21. V. Raghavan, Al–Gd-V (Aluminum-Gadolinium-Vanadium), *J. Phase Equilib. Diffus.*, 2012, **33**(1), p 62-63
22. V. Raghavan, Al-Cu-Gd (Aluminum-Copper-Gadolinium), *J. Phase Equilib. Diffus.*, 2007, **28**(6), p 547-548
23. S. Niemann and W. Jeitschko, Ternary Aluminides $A_6T_4Al_{43}$ with A = Y, Nd, Sm, Gd-Lu, Th, U and T = Cr, Mo, W, *Z. MetaIlkd.*, 1994, **85**(5), p 345-349
24. M.L. Fornasini and A. Palenzona, Crystal Structure of the Ternary $REMo_2Al_4$ Phases (RE = Gd, Er, Yb), *J. Less-Common Met.*, 1976, **45**(1), p 137-141
25. H. Okamoto, Al–Mo (Aluminum-Molybdenum), *J. Phase Equilib. Diffus.*, 2010, **31**(5), p 492-493
26. J.C. Schuster and H. Ipser, The Al-Al_8Mo_3 Section of the Binary System Aluminum-Molybdenum, *Metall. Trans. A*, 1991, **22**(8), p 1729-1736
27. M. Eumann, G. Sauthoff, and M. Palm, Re-evaluation of Phase Equilibria in the Al–Mo System, *Z. MetaIlkd.*, 2006, **97**(11), p 1502-1511
28. K.A. Gschneidner and F.W. Calderwood, The Al–Gd (Aluminum-Gadolinium) System, *Bull. Alloy Phase Diagrams*, 1988, **9**(6), p 680-683
29. A. Saccone, A.M. Cardinale, S. Delfino, and R. Ferro, Gd-Al and Dy-Al Systems: Phase Equilibria in the 0 to 66.7 at.% Al Composition Range, *Z. MetaIlkd.*, 2000, **91**(1), p 17-23
30. R.P. Elliott and F.A. Shunk, The Al–Gd (Aluminum-Gadolinium) System, *Bull. Alloy Phase Diagrams*, 1981, **2**(2), p 215-217
31. O.J.C. Runnalls and R.R. Boucher, Phase Equilibria in Aluminium-Rich Alloys of Aluminium-Gadolinium and Aluminium-Terbium, *J. Less Common Met.*, 1967, **13**(4), p 431-442
32. I. Pop, N. Dihoiu, and M. Coldea, Magnetic Behaviour of the Inter metallic System $Gd_2Ni_{17-x}Al_x$, *Philos. Mag. B*, 1979, **39**(3), p 245-252
33. L. Brewer and R.H. Lamoreaux, The Gd-Mo System (Gadolinium-Molybdenum), *J. Phase Equilib.*, 1980, **1**(2), p 78-79
34. M. Zinkevitch, N. Mattern, and K. Wetzig, Experimental Study of Ternary Fe-Gd-Mo Phase Diagram, *J. Phase Equilib.*, 1999, **20**(2), p 119-124
35. Y.N. Grin, M. Ellner, K. Peters, and J.C. Schuster, The Crystal Structures of Mo_4Al_{17} and Mo_5Al_{22}, *Z. Kristal.*, 1995, **210**(2), p 96-99
36. L. Brewer, R.H. Lamoreaux, R. Ferro, R. Marazza, and K. Girgis, *Molybdenum: Physico-chemical Properties of Its Compounds and Alloys*, Vol 7, International Atomic Energy Agency, Vienna, 1980, p 123-127
37. M. Potzschke and K. Schubert, Towards the Synthesis of Several T_4-B^3 Homologous and Quasi-Homologous System. II. The Systems Ti-Al, Zr-Al, Hf-Al, Mo-Al and Several Ternary Systems, *Z. Metallkd.*, 1962, **53**, p 548-561